Huan et al. Nanoscale Research Letters (2018) 13:246
https://doi.org/10.1186/s11671-018-2667-2

Nanoscale Research Letters

NANO REVIEW Open Access

Recent Advances in β-Ga_2O_3–Metal Contacts

Ya-Wei Huan[1], Shun-Ming Sun[1], Chen-Jie Gu[2], Wen-Jun Liu[1*], Shi-Jin Ding[1*], Hong-Yu Yu[3], Chang-Tai Xia[4] and David Wei Zhang[1]

Abstract

Ultra-wide bandgap beta-gallium oxide (β-Ga_2O_3) has been attracting considerable attention as a promising semiconductor material for next-generation power electronics. It possesses excellent material properties such as a wide bandgap of 4.6–4.9 eV, a high breakdown electric field of 8 MV/cm, and exceptional Baliga's figure of merit (BFOM), along with superior chemical and thermal stability. These features suggest its great potential for future applications in power and optoelectronic devices. However, the critical issue of contacts between metal and Ga_2O_3 limits the performance of β-Ga_2O_3 devices. In this work, we have reviewed the advances on contacts of β-Ga_2O_3 MOSFETs. For improving contact properties, four main approaches are summarized and analyzed in details, including pre-treatment, post-treatment, multilayer metal electrode, and introducing an interlayer. By comparison, the latter two methods are being studied intensively and more favorable than the pre-treatment which would inevitably generate uncontrollable damages. Finally, conclusions and future perspectives for improving Ohmic contacts further are presented.

Keywords: β-Ga_2O_3, Contacts, Metal stacks, Intermediate semiconductor layer

Introduction

Recently, gallium oxide (Ga_2O_3) has been considered as a promising candidate for preparing high-power and high-efficiency devices by virtue of its excellent material properties [1–3]. Ga_2O_3 has five different polymorphs, designated as α-Ga_2O_3, β-Ga_2O_3, γ-Ga_2O_3, δ-Ga_2O_3, and ε-Ga_2O_3, among which β-Ga_2O_3 is the most thermodynamically stable and has been extensively studied [4]. With ultra-wide bandgap of 4.6–4.9 eV [5–7], the theoretical breakdown electric field (E_{br}) of 8 MV/cm for β-Ga_2O_3 is about three times larger than that of SiC or GaN [8–10], which enables β-Ga_2O_3-based devices to handle gigantic switching voltages. The suitability of semiconductors for power device applications is usually evaluated by Baliga's figure of merit (BFOM) [11]. The BFOM of β-Ga_2O_3 is almost triple that of SiC and GaN, reducing the conduction loss significantly [3, 12–14]. Moreover, the saturation electron velocity is theoretically estimated to be around 2×10^7 cm/s, making it alluring for high-frequency operations [15–20]. Another distinctive interest of β-Ga_2O_3 among wide-bandgap semiconductors is that high-quality single crystals can be synthesized cost-effectively by using melt growth techniques [21–24]. In addition, high-quality n-type β-Ga_2O_3 epitaxial films can be realized by precisely doping with Sn, Si, Ge, and Mg, and the obtained electron density ranges from 10^{16} to 10^{19} cm^{-3} [25–28]. Because of the above-mentioned advantages over other wide-bandgap semiconductors, β-Ga_2O_3 shows its capabilities to be a promising material for power electronics as well as extreme environment (high temperature, high voltage, and high radiation) [29–31] electronics.

Many promising β-Ga_2O_3 devices have been reported, including Schottky barrier diodes [32], MOSFETs [1–3], and various types of solar-blind photodetectors [33, 34]. Among these devices, MOSFETs are the most prevailing configuration for radio frequency and high-power operation [35], giving full play to its high E_{br} and BFOM. However, one of the challenges for β-Ga_2O_3 application in MOSFET devices is the difficulty in forming Ohmic contacts compared with narrow-bandgap semiconductors [36]. Usually, an excellent Ohmic contact between the semiconductor and the metal electrode is essential for high-performance semiconductor devices [37, 38]. Low-resistance contacts could reduce the voltage drop on the contact and consequently increase the voltage

* Correspondence: wjliu@fudan.edu.cn; sjding@fudan.edu.cn
[1]State Key Laboratory of ASIC and System, School of Microelectronics, Fudan University, Shanghai 200433, China
Full list of author information is available at the end of the article

© The Author(s). 2018 **Open Access** This article is distributed under the terms of the Creative Commons Attribution 4.0 International License (http://creativecommons.org/licenses/by/4.0/), which permits unrestricted use, distribution, and reproduction in any medium, provided you give appropriate credit to the original author(s) and the source, provide a link to the Creative Commons license, and indicate if changes were made.

across the channel, securing the designed current density and high switching speeds. Furthermore, low-resistance contacts contribute to reducing heat generation which could aggravate the self-heating effect.

In consequence, the fabrication of high-quality Ohmic contacts is a prerequisite for achieving high-performance devices. In this review, we start with fundamental concepts of metal/semiconductor contacts. In the "Approaches to Ohmic Contacts" section, a summary of recent significant advances on Ohmic contacts to β-Ga_2O_3 is presented, and approaches to Ohmic contacts are discussed and analyzed. Finally, some perspectives are provided for improving Ohmic contacts to β-Ga_2O_3 in the future.

Basic Physics of Ohmic Contacts

An Ohmic contact is a metal/semiconductor junction in which there is no barrier at the interface impeding the transport of carriers, as illustrated in Fig. 1a. On the contrary, an energy barrier existing at the interface will inhibit the carrier transport between the metal and semiconductor, as is evident from Fig. 1b. Notably, the contacts formed between wide-bandgap semiconductors and metals are always Schottky. Thus, the contact resistance normally depends on the metal/semiconductor Schottky barrier height (SBH) Φ_B. For an n-type semiconductor, it obeys the equation:

$$q\Phi_B = q\Phi_m - \chi_s \quad (1)$$

where Φ_m is the work function of the metal and χ_s is the electron affinity of the semiconductor.

As depicted in Eq. (1), it is important to reduce the SBH to form the Ohmic contact. In addition, high doping in semiconductors could facilitate the formation of Ohmic contacts, e.g., for heavily doped semiconductors ($N_D > \sim 10^{18}$ cm^{-3}), the barrier will become narrow enough and allow the electrons directly to tunnel through the interface due to significant band bending of the conduction band [39], as shown in Fig. 2. Nevertheless, the doping levels that can be achieved in β-Ga_2O_3 are usually below of what can be obtained in Si, as is the case with other wide semiconductors. Other than that, the surface states also play an important role in the formation of Ohmic contacts which are frequently defined as regions of high-rate recombination. Those middle bandgap defect levels induced by the surface states are able to help the carriers transport. This implies that a good Ohmic contact can be formed by introducing proper surface states into semiconductors [40–43].

An electrical quantification of the contact characteristics is necessary to evaluate the quality of contacts. Currently, the specific contact resistivity ρ_C is one of the commonly used parameters to access the performance of Ohmic contacts, typically expressed in $\Omega \cdot cm^2$ [44]. The specific contact resistivity is a very useful quantity which is independent of the contact geometry and refers to the metal/semiconductor interface only. So far, the lowest ρ_C of 4.6×10^{-6} $\Omega \cdot cm^2$ was reported for Ti/Au contacts to β-Ga_2O_3 [45]. Wong et al. also obtained a low ρ_C of 7.5×10^{-6} $\Omega \cdot cm^2$ with Ti/Au contacts [46]. Up to now, many efforts have been devoted to obtain the contacting with low ρ_C, and the typical values for specific contact resistivities spread over a range of 10^{-5}–10^{-6} $\Omega \cdot cm^2$ for good Ohmic contacts [36].

Approaches to Ohmic Contacts

To date, investigations on the intrinsic properties of β-Ga_2O_3 mostly have been carried out on its MOSFET structure, in which two kinds of the channel synthesis method are usually adopted. One is the micromechanically exfoliated flake (nanomembrane); the other is the epitaxial β-Ga_2O_3 film on its native substrate, as summarized in Table 1.

Normally, exfoliated β-Ga_2O_3 flakes could be transferred to any substrates conveniently and cost-effectively. It is found that the material properties of β-Ga_2O_3 flakes would not degenerate during the exfoliation as evidenced by Raman spectroscopy and atomic force microscopy [19], meaning that the performance of MOSFETs based on the exfoliated flakes is comparable to that based on epitaxial layers. Due to these advantages, this method is recommended to study the electrical characteristics consisting of the density of interfacial defects, breakdown voltage, surface optical phonon scattering [47–49], and thermal property, i.e., self-heating effect [50, 51].

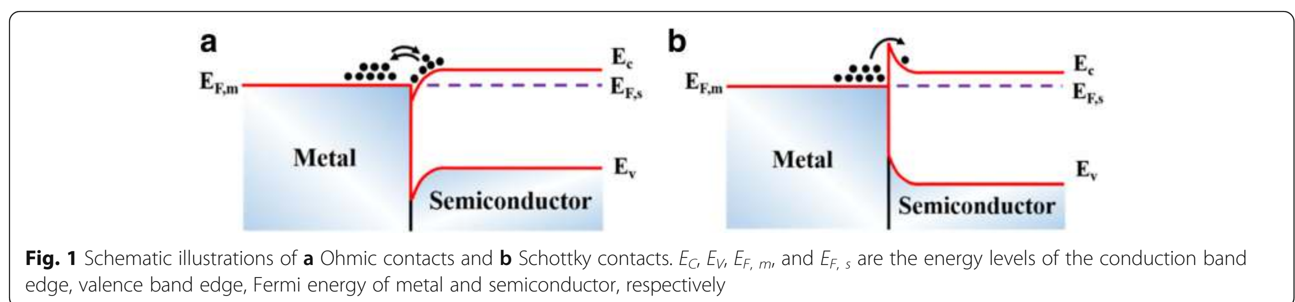

Fig. 1 Schematic illustrations of **a** Ohmic contacts and **b** Schottky contacts. E_C, E_V, $E_{F,\,m}$, and $E_{F,\,s}$ are the energy levels of the conduction band edge, valence band edge, Fermi energy of metal and semiconductor, respectively

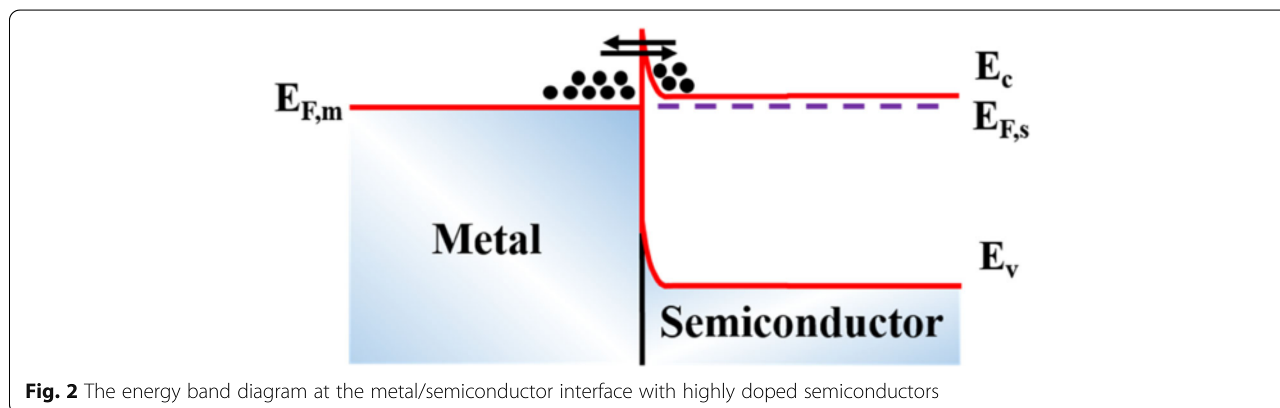

Fig. 2 The energy band diagram at the metal/semiconductor interface with highly doped semiconductors

As summarized in Table 1, methods employed to improve Ohmic contacts could be generally categorized into three types: (1) pre-treatment, (2) post-treatment, and (3) multilayer metal electrode. Besides, introducing an interlayer can also obtain superior Ohmic contacts which is not shown in Table 1.

Pre-treatment

The pre-treatment is performed before metal deposition, including ion implantation, plasma bombardment, and reactive-ion etching (RIE). Higashiwaki et al. demonstrated that the contacts formed by using Ti/Au stack with the RIE pre-treating process showed an almost Ohmic behavior, while the sample without the RIE treatment showed a Schottky behavior, as illustrated in Fig. 3 [1]. The significant difference could be attributed to the out-diffusing of the free oxygen atoms that generated through the continuous bombardment by breaking the exposed Ga–O bonds, leaving plenty of oxygen vacancies that act as donors in β-Ga_2O_3. On the other hand, the continuous RIE treatment would also generate considerable surface states which play an important role during contact formation [41]. Figure 4 shows associated DC output characteristics from which quasi-linear current at low drain voltage can be observed. In their later work, as demonstrated in Fig. 5, the output characteristics exhibited good linearity relationship between the current and drain voltage in which Si ion implantation and RIE were applied to β-Ga_2O_3 together and an extremely low specific contact resistivity of $8.1 \times 10^{-6} \Omega \cdot cm^2$ was achieved [12]. Obviously, the Ohmic behavior obtained by RIE and Si^+ implantation together would outperform that by RIE only since Si atoms are known to be shallow donors with small activation energies in β-Ga_2O_3 [34].

Table 1 The comparison of reported work about β-Ga_2O_3 MOSFETs

Channel	Carrier density/cm^{-3}	Device structure	Dielectric (method)	Process	S/D metal electrode
Flake [19]	5.5×10^{17}	BG (D-M)	285-nm SiO_2	Tube annealing	Ti/Au
Flake [88]	3×10^{17}	BG (D-M)	300-nm SiO_2	–	Ti/Au
Flake [89]	3×10^{17}	TG (E-M)	42-nm HfO_2(ALD)	–	Ti/Au
Flake [55]	3.7×10^{17}	BG (D-M)	300-nm SiO_2	RTP	Ti/Au
Flake [52]	2.7×10^{18}	BG (D/E-M)	300-nm SiO_2	Ar plasma bombardment	Ti/Al/Au
Flake [50]	8×10^{18}	BG (D/E-M)	300-nm SiO_2	Ar plasma bombardment	Ti/Al/Au
Sn-doped epilayer [12]	3×10^{17}	TG (D-M)	20-nm Al_2O_3(ALD)	Si^+ implantation(S/D) + RIE + RTP	Ti/Au
UID epilayer [57]	5×10^{19}	FP (D-M)	20-nm Al_2O_3(ALD)	Si^+ implantation (channel + S/D) + RIE + RTP	Ti/Au
Sn-doped epilayer [90]	6.34×10^{15}	TG (D/E-M)	20-nm SiO_2(ALD)	RIE + RTP	Ti/Au
Sn-doped epilayer [13]	4.8×10^{17}	TG (E-M)	20-nm Al_2O_3(ALD)	RTP	Ti/Al/Ni/Au
Sn-doped epilayer [63]	2.3×10^{17}	WG (E-M)	20-nm Al_2O_3(ALD)	RTP	Ti/Al/Ni/Au
UID epilayer [46]	$< 4 \times 10^{14}$	TG (E-M)	50-nm Al_2O_3(ALD)	Si^+ implantation(S/D) + RIE + RTP	Ti/Au
Sn-doped epilayer [53]	2×10^{17}	TG (D-M)	20-nm SiO_2 (PEALD)	Spin-on-glass doping + RTP	Ti/Au
Ge-doped epilayer [21]	4×10^{17}	TG (D-M)	20-nm Al_2O_3(ALD)	RTP	Ti/Al/Ni/Au
UID epilayer [64]	–	GR (E-M)	20-nm SiO_2(ALD)	Highly doped epitaxial cap layer on S/D + RIE + RTP	Ti/Al/Ni/Au

BG bottom gate, *TG* top gate, *DG* double gate, *FP* field plated, *WG* wrap gate, *D-M* depletion mode, *E-M* enhancement mode

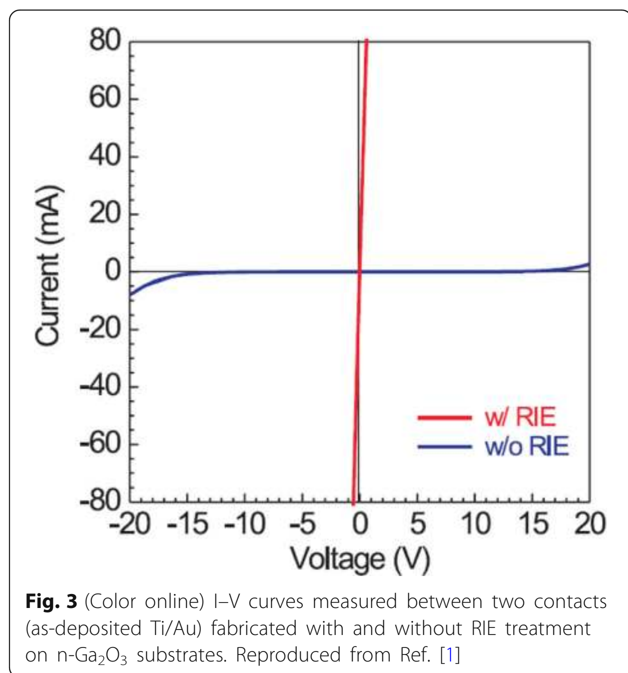

Fig. 3 (Color online) I–V curves measured between two contacts (as-deposited Ti/Au) fabricated with and without RIE treatment on n-Ga_2O_3 substrates. Reproduced from Ref. [1]

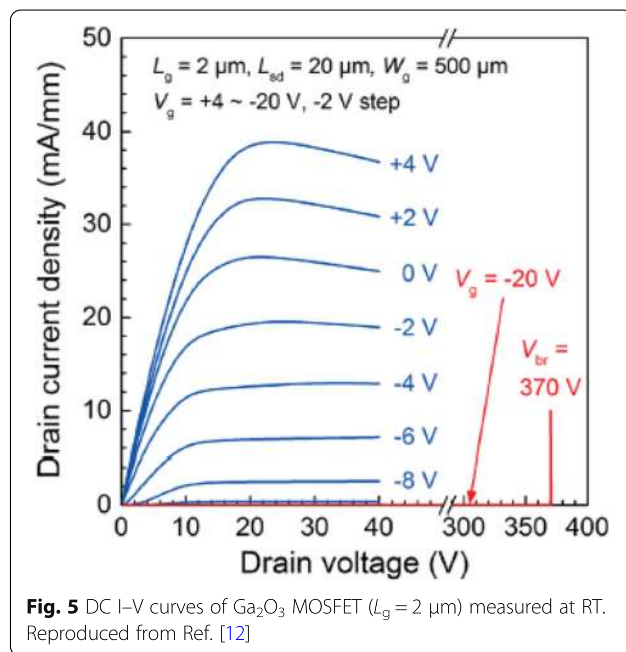

Fig. 5 DC I–V curves of Ga_2O_3 MOSFET (L_g = 2 μm) measured at RT. Reproduced from Ref. [12]

Additionally, Zhou et al. reported the high-performance β-Ga_2O_3 field-effect transistors with Ar plasma bombardment prior to contact metal deposition [52]. On the contrary, the sample without Ar bombardment exhibited Schottky contacting. The difference can be ascribed to the generation of oxygen vacancies and surface states during the Ar plasma bombardment process, the same as RIE treatment.

Although the abovementioned techniques can improve the performance of Ohmic contacts, such technologies are not practically applicable because the induced damage is usually the last thing that process engineers want in semiconductor devices, and furthermore, the damage-induced Ohmic contacts are not always reproducible.

For this reason, apart from the aforesaid traditional techniques used frequently for forming low-resistance Ohmic contacts, a relatively novel technique—spin-on-glass (SOG) doping—was recently adopted [53], and a specific contact resistivity of $2.1\pm1.4 \times 10^{-5}\Omega{\cdot}cm^2$ was achieved, which verified the effectiveness of SOG doping technique. Figure 6 shows the output characteristics of SOG-doped β-Ga_2O_3 MOSFETs which exhibited excellent linear behavior at low drain voltage. Compared with ion implantation, the SOG

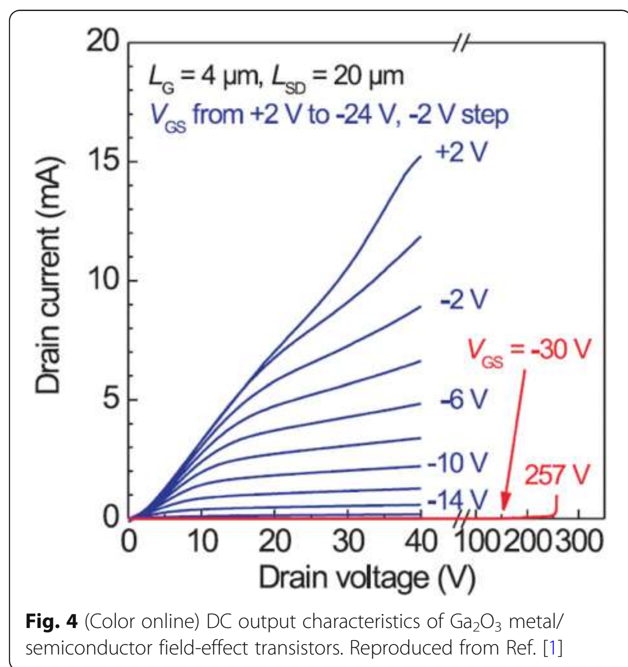

Fig. 4 (Color online) DC output characteristics of Ga_2O_3 metal/semiconductor field-effect transistors. Reproduced from Ref. [1]

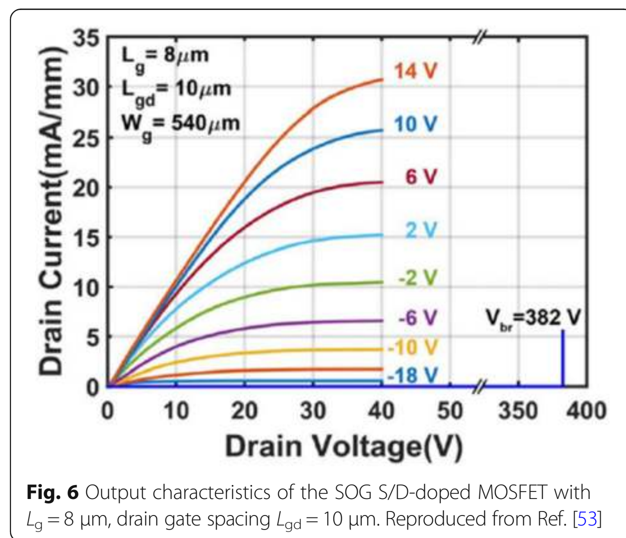

Fig. 6 Output characteristics of the SOG S/D-doped MOSFET with L_g = 8 μm, drain gate spacing L_{gd} = 10 μm. Reproduced from Ref. [53]

doping reduces damage-induced diffusion of species and lowers the costs by abandoning the expensive ion implanter. Similar to ion implantations, the basic principle behind this technology is doping the S/D region with shallow donors. Obviously, the superior Ohmic contact can be achieved with intentionally doped β-Ga_2O_3. For instance, the highly doped β-Ga_2O_3 was used to fabricate β-Ga_2O_3 field-effect transistors with drain currents exceeding 1.5 A/mm [50]. The record high drain current is due to the heavy doping in β-Ga_2O_3 which causes a very thin depletion layer, and electrons can tunnel easily across this barrier leading to an Ohmic contacting behavior. Interestingly, the orientation of the β-Ga_2O_3 surface may also exert an influence on the contacting behavior. Baik et al. reported that the same electrodes on β-Ga_2O_3 showed different contact properties, in which the sample on ($\bar{2}01$) substrate behaved as Ohmic contacts while the control sample on (010) exhibited Schottky behavior. This could be attributed to different Ga/O ratio and density of dangling bonds at specific orientations [54].

Post-treatment

The post-treatment is performed after metal deposition, mainly referring to the annealing process. Annealing plays a role in reducing damage induced by previous process technologies such as ion implantation and plasma bombardment. Additionally, it contributes to the formation of an interlayer which may reduce the conduction band discontinuity between the metal and β-Ga_2O_3. Remarkably, the parameters including temperature, atmosphere, and annealing time exert an important influence on the performance of devices. The experiment on the annealing in air and N_2 was implemented to compare the effect of annealing atmosphere on β-Ga_2O_3-based Ohmic contacts [55]. As it can be seen in Fig. 7, the performance of annealing in N_2 outperformed that in air, which could be attributed to that higher oxygen partial pressure in air suppressed the formation of oxygen vacancies. However, the dependence of contact characteristics on the temperature, atmosphere, and annealing time on contact characteristics is unclear; hence, it is further needed to optimize the parameters of the annealing process.

Multilayer Metal Electrode

Another approach to forming Ohmic contacts is to reduce the SBH at the metal/semiconductor interface. The SBH equals the difference between the work function of the metal and the electron affinity of the semiconductor. Based on this recognition, one might expect that metals with low work function would form Ohmic contacts on β-Ga_2O_3. Nevertheless, it has been proven that the work function is not the dominant factor of forming Ohmic contact [56].

Nine metals deposited on β-Ga_2O_3 were selected based on the properties such as work function, melting temperature, and oxide stability [57]. The metal work function of Ti and electron affinity of unintentionally doped β-Ga_2O_3 are known to be 4.33 eV and 4.00 ±0.05 eV, respectively [19, 58, 59], so a barrier of 0.22 eV should exist at the interface leading to the Schottky contact. Nonetheless, it turned out that Ti contacts with an Au capping layer were Ohmic with the lowest resistance among nine metals after annealing. In the meanwhile, Bae et al. explored the dependence of contact properties on the Ti/Au and Ni/Au for devices based on the exfoliated β-Ga_2O_3 flakes [55]. It was observed that the performance of MOSFETs with Ti/Au metal electrodes outperformed those with Ni/Au metal electrodes under the same annealing condition. At the beginning, it was considered that the work functions of Ni and Ti are 5.01 eV and 4.33 eV, respectively, so Ti may form an Ohmic contact more easily than Ni; however, studies through the energy dispersive spectroscopy (EDS) demonstrated that the oxygen atomic percentage in the β-Ga_2O_3 region decreased while the oxygen atomic percentage in Ti near the interface increased after annealing, as illustrated in Fig. 8 [55]. This phenomenon is ascribed to the out-diffusion of oxygen atoms from

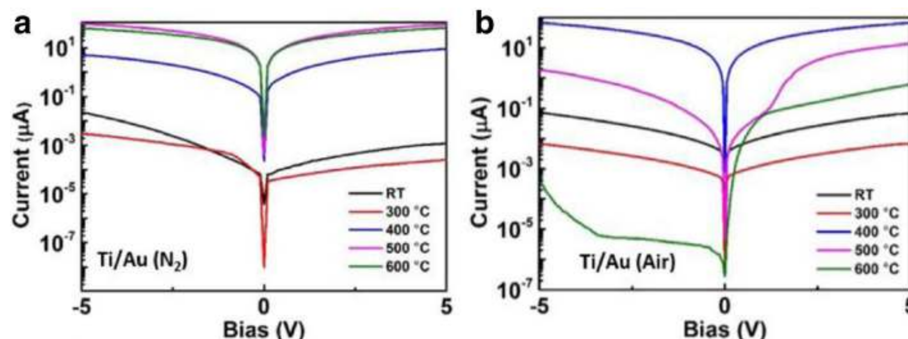

Fig. 7 Electrical properties of β-Ga_2O_3 flakes with different thermal annealing atmosphere and annealing temperature. Ti/Au contacts under **a** N_2 and **b** air. Reproduced from Ref. [55]

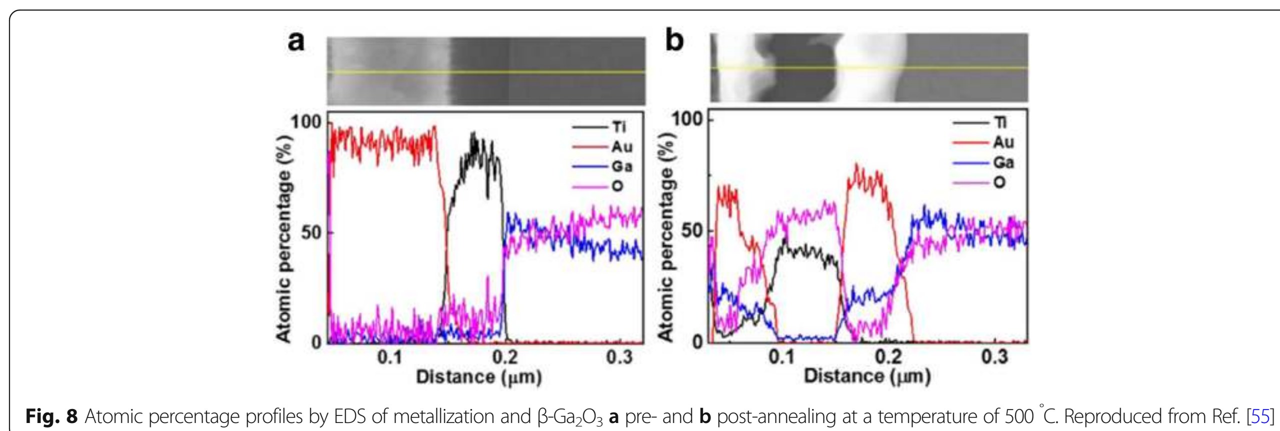

Fig. 8 Atomic percentage profiles by EDS of metallization and β-Ga_2O_3 **a** pre- and **b** post-annealing at a temperature of 500 °C. Reproduced from Ref. [55]

β-Ga_2O_3 into Ti metal, leading to the formation of oxygen vacancies acting as donors. Moreover, during the annealing process, the accelerated out-diffusion of oxygen atoms in β-Ga_2O_3 could react with Ti and form Ti_2O_3 which is useful for forming Ohmic contacts owing to its low work function (3.6–3.9 eV). Therefore, the interfacial reaction between metals and β-Ga_2O_3 is an important factor in forming Ohmic contacts at the metal/semiconductor interface.

In addition, it is found that most Ti/Au metal electrodes used to form Ohmic contacts were annealed at 450 °C [45, 53] or 470 °C [12, 46, 57, 60] by rapid thermal process. A similar degradation behavior of contact characteristics was observed when the annealing was performed above 500 °C in Ref. [55, 56], as illustrated in Figs. 7 and 9, respectively. Yao et al. speculated that an insulating oxide layer was formed possibly at elevated annealing temperature, resulting in the deteriorated contacts. Nevertheless, Bae et al. observed that the surface of deposited metal was much rougher after 700 °C annealing due to the intermixing of metals and the diffusion of gallium and oxygen atoms into metal electrodes, which was ascribed as the reason for degradation behavior. Obviously, the degradation mechanisms of Ti/Au contacts to β-Ga_2O_3 after high-temperature annealing are still under debate.

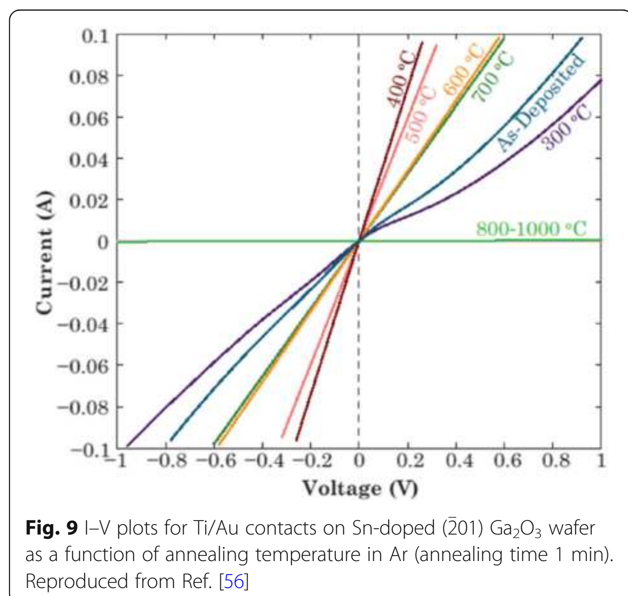

Fig. 9 I–V plots for Ti/Au contacts on Sn-doped ($\bar{2}01$) Ga_2O_3 wafer as a function of annealing temperature in Ar (annealing time 1 min). Reproduced from Ref. [56]

β-Ga_2O_3-based devices with Ti/Au contacts cannot meet the demand for working under high temperature. Hence, to avoid the degradation of contact characteristics at elevated annealing temperature, more complex metal stacks should be adopted. By far, Ti/Al/Au [50, 52], Ti/Au/Ni [61, 62], and Ti/Al/Ni/Au metal stacks [13, 21, 63, 64] have been employed to form electrical contacts on β-Ga_2O_3. But a comprehensive comparison of contact characteristics between these metal stacks is still insufficient.

Mohammad [65] and Greco et al. [36] discussed the role of each metal layer in the complex metal stacks, providing some guidelines for improving the Ohmic contacts. The schematic of the metal stacks is shown in Fig. 10. Note that this approach is currently developing for GaN-based power devices [66–69].

The first metal layer on the substrate, referred to as contact layer, should have a low work function and good adhesion to the substrate. Moreover, it may also block the diffusion of upper layer metals with large work functions into the substrate. Presently, Ti is the principal metal as contact layer to β-Ga_2O_3 because of its low function (4.33 eV) and good adhesion to the substrate. Besides, the formation of Ti_2O_3 and Ti_3O_5 with lower work functions than Ti at the interface is favored in forming Ohmic contacts since the oxides reduce the SBH and leave behind oxygen vacancies acting as donors. However, other metals with low work functions including Ta (3.1 eV) and Hf (3.9 eV) have not been explored yet. The second overlayer with a low work function should be able to form intermetallic compounds with the contact layer to prevent their diffusion

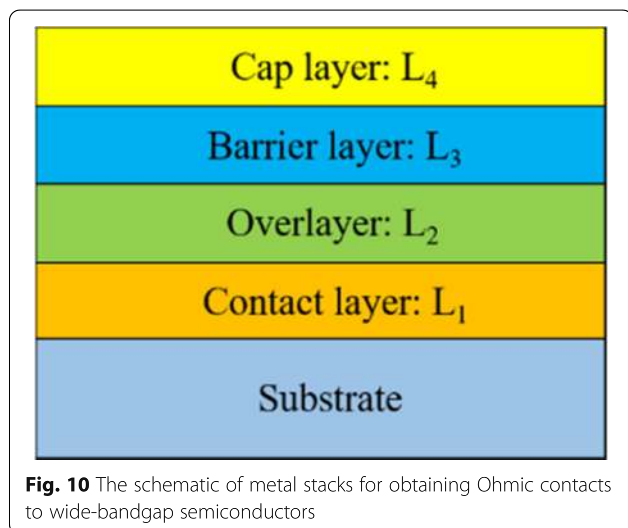

Fig. 10 The schematic of metal stacks for obtaining Ohmic contacts to wide-bandgap semiconductors

into the interface. Presently, Al is used as the overlayer since it can meet these requirements. The third metal layer (barrier layer) serves the purpose of limiting the in-diffusion of the upper metal layer and out-diffusion of lower metal layers [70, 71]. Ni is the most commonly used barrier layer for β-Ga_2O_3. There are other good candidates like Mo, Nb, and Ir with high melting points to substitute Ni which are expected to have lower reactivity and solubility for Au than Ni [72–75]. The fourth cap layer acts as a protective layer to prevent or minimize the oxidation of underlying metals. Practically, Au is commonly employed to serve this purpose.

Introducing an Interlayer

There are mainly two methods of introducing an interlayer at the metal/β-Ga_2O_3 interface. One is to form an intermediate semiconductor layer (ISL) with low work function by annealing, e.g., Ti_2O_3. The other is to insert the deposited ISL between the metal and β-Ga_2O_3, which has been intensively studied [76–78]. Compared with the former method, the latter is more favorable to form Ohmic contacts owing to the high carrier concentration of ISL. The bandgaps of ISLs range from 3.5 to 4.0 eV [79–81], like AZO (~ 3.2 eV) [82], In_2O_3 (~ 2.9 eV) [83, 84], and IGZO (~ 3.5 eV) [85]. Typically, the SBHs of various metals deposited on β-Ga_2O_3 are in the range of 0.95–1.47 eV [86, 87], as shown in Fig. 11a. Nonetheless, the incorporation of a thin ISL reduces the SBH, making it easier for electrons to transport from the metal to the conduction band of β-Ga_2O_3, as illustrated in Fig. 11b. Additionally, the high density of electrons in ISL could further reduce the contact resistance.

Lately, AZO/Ti/Au was used as electrodes on Si^+-implanted β-Ga_2O_3, and the obtained specific contact resistivity was 2.82 × 10^{-5} Ω·cm^2 after annealing [76]. Oshima et al. achieved platinum/indium–tin oxide (Pt/

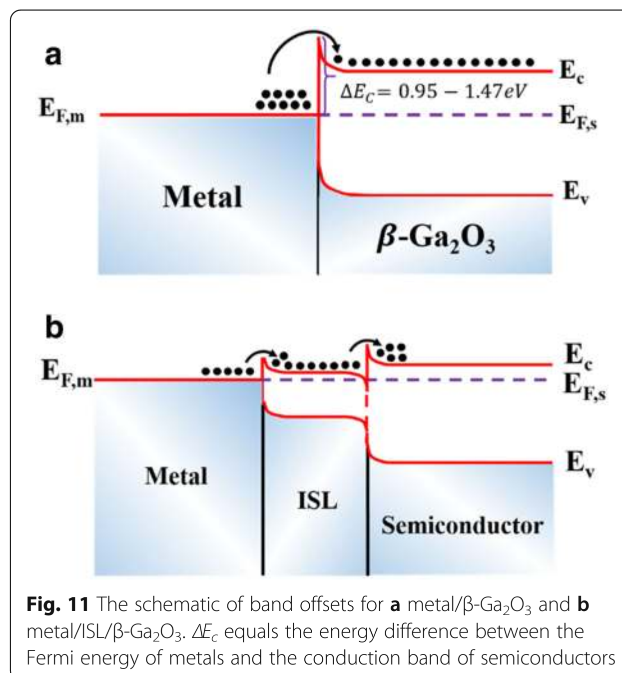

Fig. 11 The schematic of band offsets for **a** metal/β-Ga_2O_3 and **b** metal/ISL/β-Ga_2O_3. ΔE_c equals the energy difference between the Fermi energy of metals and the conduction band of semiconductors

ITO) Ohmic contacts to β-Ga_2O_3 with a wide range of process temperature window [77]. The large process window of 900–1150 °C enables the realization of high-temperature operation. And ITO/Ti/Au electrodes to β-Ga_2O_3 were also demonstrated by Carey et al. [78] in which the sample showed Ohmic behavior with ρ_C of 6.3 × 10⁻5 Ω·cm^2 after annealing. Without the ITO, the same annealing did not deliver linear current–voltage characteristics. These results verify the effectiveness of adding ISL for obtaining Ohmic contacts.

Notably, a bubble on the surface of ITO/Ti/Au contacts was observed while no bubbling on the single ITO layer without metal layer above [78]. It was considered as the result of out-diffusion of oxygen atoms in the ITO layer into the upper metal layers. Hence, it is necessary to choose appropriate metal or metal stacks as capping layers on ITO to prevent the degradation of surface morphology.

Conclusions

In this work, we have summarized the significant progress in R&D of β-Ga_2O_3 MOSFETs. Nevertheless, the contacts on β-Ga_2O_3 are one of the key issues limiting its potential application as high-frequency and high-voltage devices in the future. Although this review provides an overview of the state-of-the-art methods for forming Ohmic contacts, there is still much space left to be explored, and a set of concise prospects can be digested as follows: (i) The temperature dependence and degradation mechanism of contact characteristics need further investigations for clear clarification; (ii) Metals with low work function like Ta and Hf and metals with

high melting point like Mo, Nb, and Ir are worthy to be screened for serving as the contact layer and barrier layer, respectively; (iii) The optimal metal stacks on β-Ga_2O_3 have not been fully realized yet, and a comprehensive and systematic study of metal stacks to β-Ga_2O_3 is imperative for achieving low-resistance and thermally stable Ohmic contacts; and (iv) Other potential ISLs consisting of ZnO, IZO, IGZO, etc. remain unexploited, as well as the influence of varying thickness and proportion of ingredients of ISLs on the performance of the contacts. In summary, the studies about Ohmic contacts to β-Ga_2O_3 are still quite superficial; we believe that this topic will continue to be one of the focused issues in the future. Hopefully, the approaches to forming Ohmic contacts presented in this review would be instrumental in achieving high-performance β-Ga_2O_3 devices.

Funding
This work was supported in part by the National Natural Science Foundation of China (Grant Nos. 61474027, 61774041, and 11604169), in part by the National Key Technologies Research and Development Program of China (Grant Nos. 2015ZX02102–003 and 2017YFB0405600), and in part by Shanghai Pujiang Program, China (Grant No. 16PJ1400800).

Availability of Data and Materials
The datasets supporting the conclusions of this manuscript are included within the manuscript.

Authors' Contributions
YWH and SMS conducted the extensive literature review and analyzed the data. WJL and SJD supervised the project and wrote the manuscript. CJG, HYY, CTX, and DWZ helped to review and discuss the manuscript. All authors read and approved the final manuscript.

Competing Interests
The authors declare that they have no competing interests.

Publisher's Note

Springer Nature remains neutral with regard to jurisdictional claims in published maps and institutional affiliations.

Author details
[1]State Key Laboratory of ASIC and System, School of Microelectronics, Fudan University, Shanghai 200433, China. [2]Division of Microelectronics, School of Science, Ningbo University, Ningbo 315211, China. [3]Department of Electrical and Electronic Engineering, Southern University of Science and Technology, Shenzhen 518055, China. [4]Key Laboratory of Materials for High Power Laser, Shanghai Institute of Optics and Fine Mechanics, Chinese Academy of Science, Shanghai 201800, China.

Received: 23 June 2018 Accepted: 10 August 2018
Published online: 22 August 2018

References

1. Higashiwaki M, Sasaki K, Kuramata A, Masui T, Yamakoshi S (2012) Gallium oxide (Ga_2O_3) metal-semiconductor field-effect transistors on single-crystal β-Ga_2O_3 (010) substrates. Appl Phys Lett 100(1):013504
2. Higashiwaki M, Murakami H, Kumagai Y, Kuramata A (2016) Current status of Ga_2O_3 power devices. Jpn J Appl Phys 55(12):1202A1
3. Higashiwaki M, Sasaki K, Murakami H, Kumagai Y, Koukitu A, Kuramata A et al (2016) Recent progress in Ga_2O_3 power devices. Semicond Sci Technol 31(3):034001
4. Roy R, Hill VG, Osborn EF (1952) Polymorphism of Ga_2O_3 and the system Ga_2O_3–H_2O. J Am Chem Soc 74:719–722
5. Tippins HH (1965) Optical absorption and photoconductivity in the band edge of β-Ga_2O_3. Phys Rev 140:A316–A319
6. Stepanov SI, Nikolaev VI, Bougrov VE, Romanov AE (2016) Gallium oxide: properties and applications-a review. Rev Adv Mater Sci 44:63–86
7. He H, Orlando R, Blanco MA, Pandey R, Amzallag E, Baraille I et al (2006) First-principles study of the structural, electronic, and optical properties of Ga_2O_3 in its monoclinic and hexagonal phases. Phys Rev B 74(19):195123
8. Higashiwaki M, Sasaki K, Kamimura T, Wong M, Krishnamurthy D, Kuramata A et al (2013) Depletion-mode Ga_2O_3 metal-oxide-semiconductor field-effect transistors on β-Ga_2O_3 (010) substrates and temperature dependence of their device characteristics. Appl Phys Lett 103(12):123511
9. Green AJ, Chabak KD, Heller ER, Fitch RC, Baldini M, Fiedler A et al (2016) 3. 8-MV/cm breakdown strength of MOVPE-grown Sn-doped β-Ga_2O_3 MOSFETs. IEEE Electron Device Lett 37(7):902–905
10. Yan X, Esqueda IS, Ma J, Tice J, Wang H (2018) High breakdown electric field in β-Ga_2O_3/graphene vertical barristor heterostructure. Appl Phys Lett 112(3):032101
11. Higashiwaki M, Jessen GH (2018) Guest editorial: the dawn of gallium oxide microelectronics. Appl Phys Lett 112:060401
12. Higashiwaki M, Kuramata A, Murakami H, Kumagai Y (2017) State-of-the-art technologies of gallium oxide power devices. J Phys D Appl Phys 50(33):333002
13. Pearton SJ, Yang J, Cary PH, Ren F, Kim J, Tadjer MJ et al (2018) A review of Ga_2O_3 materials, processing, and devices. Appl Phys Rev 5(1):011301
14. Mastro MA, Kuramata A, Calkins J, Kim J, Ren F, Pearton SJ (2017)) Perspective—opportunities and future directions for Ga_2O_3. ECS J Solid State Sci Technol 6(5):356–359
15. Hwang WS, Verma A, Peelaers H, Protasenko V (2014) High-voltage field effect transistors with wide-bandgap β-Ga_2O_3 nanomembranes. Appl Phys Lett 104(20):203111
16. Wong MH, Sasaki K, Kuramata A, Yamakoshi S, Higashiwaki M (2016) Electron channel mobility in silicon-doped Ga_2O_3 MOSFETs with a resistive buffer layer. Jpn J Appl Phys 55(12):1202B9
17. Moser N, McCandless J, Crespo A, Leedy K, Green A, Neal A et al (2017) Ge-doped β-Ga_2O_3 MOSFETs. IEEE Electron Device Lett 38(6):775–778
18. Víllora EG, Shimamura K, Ujiie T, Aoki K (2008) Electrical conductivity and lattice expansion of β-Ga_2O_3 below room temperature. Appl Phys Lett 92(20):A316
19. Parisini A, Fornari R (2016) Analysis of the scattering mechanisms controlling electron mobility in β-Ga_2O_3 crystals. Semicond Sci Technol 31(3):035023
20. Ma N, Tanen N, Verma A, Guo Z, Luo T, Xing H et al (2016) Intrinsic electron mobility limits in β-Ga_2O_3. Appl Phys Lett 109(21):212101
21. Víllora EG, Shimamura K, Yoshikawa Y, Aoki K, Ichinose N (2004) Large-size β-Ga_2O_3 single crystals and wafers. J Cryst Growth 270(3–4):420–426
22. Aida H, Nishiguchi K, Takeda H, Aota N, Sunakawa K, Yaguchi Y (2008) Growth of β-Ga_2O_3 single crystals by the edge-defined, film fed growth method. Jpn J Appl Phys 47(11):8506–8509
23. Tomm Y, Reiche P, Klimm D, Fukuda T (2000) Czochralski grown Ga_2O_3 crystals. J Cryst Growth 220(4):510–514
24. Galazka Z, Uecker R, Irmscher K, Albrecht M, Klimm D, Pietsch M et al (2010) Czochralski growth and characterization of β-Ga_2O_3 single crystals. Cryst Res Technol 45(12):1229–1236
25. Higashiwaki M, Sasaki K, Kuramata A, Masui T, Yamakoshi S (2014) Development of gallium oxide power devices. Phys Status Solidi A 211(1):21–26
26. Baldini M, Galazka Z, Wagner G (2018) Recent progress in the growth of β-Ga_2O_3 for power electronics applications. Mater Sci Semicond Process 78:132–146
27. Suzuki N, Ohira S, Tanaka M, Sugawara T, Nakajima K, Shishido T (2007) Fabrication and characterization of transparent conductive Sn-doped β-Ga_2O_3 single crystal. Phys Status Solidi C 4(7):2310–2313
28. Chikoidze E, Fellous A, Perez-Tomas A, Sauthier G, Tchelidze T, Ton-That C et al (2017) P-type β-gallium oxide: a new perspective for power and optoelectronic devices. Mater Today Phys 3:118–126
29. Yang G, Jang S, Ren F, Pearton SJ, Kim J (2017) Influence of high-energy proton irradiation on β-Ga_2O_3 nanobelt field-effect transistors. ACS Appl Mater Inter 9(46):1–23
30. Wong MH, Takeyama A, Makino T, Ohshima T, Sasaki K, Kuramata A et al (2018) Radiation hardness of β-Ga_2O_3 metal-oxide-semiconductor field-effect transistors against gamma-ray irradiation. Appl Phys Lett 112(2):023503
31. Yang J, Chen Z, Ren F, Pearton SJ, Yang G, Kim J et al (2018) 10 MeV proton damage in β-Ga_2O_3 Schottky rectifiers. J Vac Sci Technol B 36(1):011206
32. Sasaki K, Higashiwaki M, Kuramata A, Masui T (2013) Schottky barrier diodes fabricated by using single-crystal β-Ga_2O_3 (010) substrates. IEEE Electron Device Lett 34(4):493–495

33. Oh S, Mastro MA, Tadjer MJ, Kim J (2017) Solar-blind metal-semiconductor-metal photodetectors based on an exfoliated β-Ga_2O_3 micro-flake. ECS J Solid State Sci Technol 6(8):Q79–Q83
34. Oshima T, Okuno T, Arai N, Suzuki N, Ohira S, Fujita S (2008) Vertical solar-blind deep-ultraviolet Schottky photodetectors based on β-Ga_2O_3 substrates. Appl Phys Exp 1(1):011202
35. Green AJ, Chabak KD, Baldini M, Moser N, Gilbert RC, Fitch R et al (2017) β-Ga2O3 MOSFETs for radio frequency operation. IEEE Electron Device Lett 38(6):790–793
36. Greco G, Iucolano F, Roccaforte F (2016) Ohmic contacts to gallium nitride materials. Appl Surf Sci 383:324–345
37. Murakami M, Koide Y (1998) Ohmic contacts for compound semiconductors. Crit Rev Solid State Mater Sci 23(1):1–60
38. Diemer G (1956) Nature of an ohmic metal-semiconductor contact. Phys Rev 103(2):279
39. Chang CY, Sze SM (1970) Carrier transport across metal-semiconductor barriers. Solid State Electron 13(6):727–740
40. Cowley AM, Sze SM (1965) Surface states and barrier height of metal-semiconductor systems. J Appl Phys 36(10):3212–3220
41. Bardeen J (1947) Surface states and rectification at a metal semi-conductor contact. Phys Rev 71(10):717–727
42. Rideout VL (1975) A review of the theory and technology for Ohmic contacts to group III–V compound semiconductors. Solid State Electron 18(6):541–550
43. Shen TC, Gao GB, Morkoc H (1992) Recent developments in ohmic contacts for III–V compound semiconductors. J Vac Sci Technol B 10(5):2113–2132
44. Ng KK, Liu R (1990) On the calculation of specific contact resistivity on ⟨100⟩ Si. IEEE Trans Electron Devices 37(6):1535–1537
45. Sasaki K, Higashiwaki M, Kuramata A, Masui T, Yamakoshi S (2013) Si-ion implantation doping in β-Ga_2O_3 and its application to fabrication of low-resistance Ohmic contacts. Appl Phys Exp 6(4):086502
46. Wong MH, Nakata Y, Kuramata A, Yamakoshi S, Higashiwaki M (2017) Enhancement-mode Ga_2O_3 MOSFETs with Si-ion-implanted source and drain. Appl Phys Exp 10(4):041101
47. Mohamed M, Janowitz C, Unger I, Manzke R, Galazka Z, Uecker R et al (2010) The electronic structure of β-Ga_2O_3. Appl Phys Lett 97(21):081906
48. Oh JG, Hong SK, Kim CK, Bong JH, Shin J, Choi SY et al (2014) High performance graphene field effect transistors on an aluminum nitride substrate with high surface phonon energy. Appl Phys Lett 104(19):193112
49. Bhattacharjee S, Ganapathi KL, Chandrasekar H, Paul T, Mohan S, Ghosh A et al (2017) Nitride dielectric environments to suppress surface optical phonon dominated scattering in high-performance multilayer MoS_2 FETs. Adv Electron Mater 3(1):1600358
50. Zhou H, Maize K, Qiu G, Shakouri A, Ye PD (2017) β-Ga_2O_3 on insulator field-effect transistors with drain currents exceeding 1.5A/mm and their self-heating effect. Appl Phys Lett 111(9):092102
51. Zhou H, Maize K, Noh J, Shakouri A, Ye PD (2017) Thermodynamic studies of β-Ga_2O_3 nanomembrane field-effect transistors on a sapphire substrate. ACS Omega 2(11):7723–7729
52. Zhou H, Si M, Alghamdi S, Qiu G, Yang L, Ye PD (2016) High-performance depletion/enhancement-mode β-Ga_2O_3 on insulator (GOOI) field-effect transistors with record drain currents of 600/450 mA/mm. IEEE Electron Device Lett 38(1):103–106
53. Zeng K, Wallace JS, Heimburger C, Sasaki K, Kuramata A, Masui T et al (2017) Ga_2O MOSFETs using spin-on-glass source/drain doping technology. IEEE Electron Device Lett 38(4):513–516
54. Janga S, Jung S, Beers K, Yang J, Ren F, Kuramata A et al (2017) A comparative study of wet etching and contacts on ($\bar{2}$01) and (010) oriented β-Ga_2O_3. J Alloys Compd 731:118
55. Bae J, Kim HY, Kim J (2017) Contacting mechanically exfoliated β-Ga_2O_3 nanobelts for (opto)electronic device applications. ECS J Solid State Sci Technol 6(2):Q3045–Q3048
56. Yao Y, Davis RF, Porter LM (2017) Investigation of different metals as Ohmic contacts to β-Ga_2O_3: comparison and analysis of electrical behavior, morphology, and other physical properties. J Electron Mater 46(4):2053–2060
57. Wong MH, Sasaki K, Kuramata A, Yamakoshi S (2015) Field-plated Ga_2O_3 MOSFETs with a breakdown voltage of over 750 V. IEEE Electron Device Lett 37(2):212–215
58. Wheeler VD, Shahin DI, Tadjer MJ, Eddy CR Jr (2017) Band alignments of atomic layer deposited ZrO_2 and HfO_2 high-k dielectrics with (−201) β-Ga_2O_3. ECS J Solid State Sci Technol 6(2):Q3052–Q3055
59. Mohamed M, Irmscher K, Janowitz C, Galazka Z (2012) Schottky barrier height of Au on the transparent semiconducting oxide β-Ga_2O_3. Appl Phys Lett 101(13):132106
60. Wong MH, Sasaki K, Kuramata A, Yamakoshi S, Higashiwaki M (2015) Anomalous Fe diffusion in Si-ion-implanted β-Ga_2O_3 and its suppression in Ga_2O_3 transistor structures through highly resistive buffer layers. Appl Phys Lett 106(3):032105
61. Krishnamoorthy S, Xia Z, Bajaj S, Brenner M, Rajan S (2017) Delta-doped β-gallium oxide field effect transistor. Appl Phys Exp 10(5):051102
62. Krishnamoorthy S, Xia Z, Joishi C, Zhang Y, McGlone J, Johnson J et al (2017) Modulation-doped β-$(Al_{0.2}Ga_{0.8})_2O_3$/Ga_2O_3 field-effect transistor. Appl Phys Lett 111(2):023502
63. Chabak KD, Moser N, Green AJ, Walker DE Jr, Tetlak SE, Heller E et al (2016) Enhancement-mode Ga_2O_3 wrap-gate fin field-effect transistors on native (100) β-Ga_2O_3 substrate with high breakdown voltage. Appl Phys Lett 109(21):213501
64. Chabak K, Green A, Moser N, Tetlak S, McCandless J, Leedy K et al (2017) Gate-recessed, laterally-scaled β-Ga_2O_3 MOSFETs with high-voltage enhancement-mode operation. 75th Annual Device Research Conference (DRC), pp 1–2
65. Mohammad SN (2004) Contact mechanisms and design principles for alloyed Ohmic contacts to p-type GaN. J Appl Phys 95(9):4856–4865
66. Chiu YS, Lin TM, Nguyen HQ, Weng YC (2014) Ti/Al/Ti/Ni/Au ohmic contacts on AlGaN/GaN high electron mobility transistors with improved surface morphology and low contact resistance. J Vac Sci Technol B 32(1):011216
67. Iucolano F, Roccaforte F, Alberti A, Bongiorno C (2006) Temperature dependence of the specific resistance in Ti / Al / Ni / Au contacts on n-type GaN. J Appl Phys 100(12):123706
68. Ruvimov S, Liliental-Weber Z, Washburn J, Duxstad KJ, Haller EE, Fan ZF et al (1996) Microstructure of Ti/Al and Ti/Al/Ni/Au ohmic contacts for n-GaN. Appl Phys Lett 69(11):1556–1558
69. Chen ZZ, Qin ZX, Hu CY, Hu XD, Yu TJ, Tong YZ et al (2014) Ohmic contact formation of Ti/Al/Ni/Au to n-GaN by two-step annealing method. Mater Sci Eng B 111(1):36–39
70. Mohammed FM, Wang L, Adesida I, Piner E (2006) The role of barrier layer on Ohmic performance of Ti/Al-based contact metallizations on AlGaN/GaN heterostructures. J Appl Phys 100(2):023708
71. Qin ZX, Chen ZZ, Tong YZ, Ding XM, Hu XD, Yu TJ et al (2004) Study of Ti/Au, Ti/Al/Au, and Ti/Al/Ni/Au ohmic contacts to n-GaN. Appl Phys A Mater Sci Process 78(5):729–731
72. Khanna R, Gila BP, Stafford L, Pearton SJ, Ren F, Kravchenko II (2007) Ir-based Schottky and Ohmic contacts on n-GaN. J Electrochem Soc 154(7):H584–H588
73. Kumar V, Zhou L, Selvanathan D, Adesida I (2002) Thermally-stable low-resistance Ti/Al/Mo/Au multilayer ohmic contacts on n–GaN. J Appl Phys 92(3):1712–1714
74. Fitch RC, Gillespie JK, Moser N, Jenkins T, Sewell J, Via D et al (2004) Properties of Ir-based Ohmic contacts to AlGaN/GaN high electron mobility transistors. Appl Phys Lett 84(9):1495–1497
75. Nakayama T, Miyamoto H, Ando Y, Okamoto Y, Inoue T, Hataya K et al (2004) Low-contact-resistance and smooth-surface Ti/Al/Nb/Au ohmic electrode on AlGaN/GaN heterostructure. Appl Phys Lett 85(17):3775–3776
76. Carey PH, Yang J, Ren F, Hays DC, Pearton SJ, Jang S et al (2017) Ohmic contacts on n-type β-Ga_2O_3 using AZO/Ti/Au. AIP Adv 7(9):095313
77. Oshima T, Wakabayashi R, Hattori M, Hashiguchi A, Kawano N, Sasaki K et al (2016) Formation of indium–tin oxide ohmic contacts for β-Ga_2O_3. Jpn J Appl Phys 55(12):1202B7
78. Carey PH, Yang J, Ren F, Hays DC, Pearton SJ, Jang S et al (2017) Improvement of Ohmic contacts on Ga_2O_3 through use of ITO-interlayers. J Vac Sci Technol B 35(6):061201
79. Kumar B, Gong H, Akkipeddi R (2005) High mobility undoped amorphous indium zinc oxide transparent thin films. J Appl Phys 98(7):073703
80. Hosono H (2007) Recent progress in transparent oxide semiconductors: materials and device application. Thin Solid Films 515(15):6000–6014
81. Min JK, Kim TG (2016) Fabrication of metal-deposited indium tin oxides: its applications to 385 nm light-emitting diodes. ACS Appl Mater Inter 8(8):5453–5457
82. Walsh A, Da SJ, Wei SH (2011) Multi-component transparent conducting oxides: progress in materials modelling. J Phys Condens Matter 23(33):334210
83. Walsh A, Da Silva JLF, Wei SH, Körber C, Klein A, Piper LFJ et al (2008) Nature of the band gap of In_2O_3 revealed by first-principles calculations and X-ray spectroscopy. Phys Rev Lett 100(16):167402

84. Liu H, Avrutin V, Izyumskaya N, Özgür Ü, Morkoç H (2010) Transparent conducting oxides for electrode applications in light emitting and absorbing devices. Superlattice Microst 48(5):458–484
85. Hosono H, Nomura K, Ogo Y, Uruga T, Kamiya T (2008) Factors controlling electron transport properties in transparent amorphous oxide semiconductors. J Non-Cryst Solids 354(19–25):2796–2800
86. Oh S, Jung Y, Mastro MA, Hite JK, Eddy CR, Kim J (2015) Development of solar-blind photodetectors based on Si-implanted β-Ga_2O_3. Opt Express 23(22):28300
87. Armstrong AM, Crawford MH, Jayawardena A, Ahyi A, Dhar S (2016) Role of self-trapped holes in the photoconductive gain of β-gallium oxide Schottky diodes. J Appl Phys 119(10):103102
88. Kim J, Oh S, Mastro MA, Kim J (2016) Exfoliated β-Ga_2O_3 nano-belt field-effect transistors for air-stable high power and high temperature electronics. Phys Chem Chem Phys 18(23):15760–15764
89. Tadjer MJ, Mahadik NA, Wheeler VD, Glaser ER, Ruppalt L, Koehler AD et al (2016) Editors' choice communication—a (001) β-Ga_2O_3 MOSFET with +2.9 V threshold voltage and HfO_2 gate dielectric. ECS J Solid State Sci Technol 5(9):468–470
90. Zeng K, Sasaki K, Kuramata A, Masui T, Singisetti U (2016) Depletion and enhancement mode β-Ga_2O_3 MOSFETs with ALD SiO_2 gate and near 400 V breakdown voltage. 74th Annual Device Research Conference (DRC), pp 1–2

Submit your manuscript to a SpringerOpen journal and benefit from:

- ► Convenient online submission
- ► Rigorous peer review
- ► Open access: articles freely available online
- ► High visibility within the field
- ► Retaining the copyright to your article

Submit your next manuscript at ► springeropen.com